*Inorg. Chem.* **2007**, *46*, 9415–9424


# Trapping of Anionic Organic Radicals by $(Tp^{Me2})_2Ln$ (Ln = Sm, Eu)

**Ângela Domingos,[†] Irene Lopes,[†] João C. Waerenborgh,[†] Noémia Marques,[†] G. Y. Lin,[‡] X. W. Zhang,[‡] Josef Takats,[‡] Robert McDonald,[‡] Anna C. Hillier,[§] Andrea Sella,*[,§] Mark R. J. Elsegood,[||] and Victor W. Day[⊥]**

*Departamento de Química, ITN, Estrada Nacional 10, 2686-953, Sacavém, Portugal, Department of Chemistry, University of Alberta, Edmonton, Alberta T6G 2G2, Canada, Christopher Ingold Laboratories, Department of Chemistry, University College London, 20 Gordon Street, London, WC1H 0AJ, United Kingdom, Chemistry Department, Loughborough University, Loughborough, Leicestershire, LE11 3TU, United Kingdom, and Department of Chemistry, University of Kansas, 1251 Wescoe Hall Drive, Lawrence, Kansas 66045*

Received July 10, 2007

Stoichiometric reaction of $[Sm(Tp^{Me2})_2]$, **1**, with a variety of reducible ketone- and quinone-type substrates gave thermally stable, isolable radical anions/ketyls in moderate to good yields. Thus reaction with benzophenone gave $[Sm(Tp^{Me2})_2(OCPh_2)]$, **2**, with fluorenone $[Sm(Tp^{Me2})_2(\eta^1\text{-}OC_{13}H_8)]$, **3**, and di-*tert*-butylparaquinone $[Sm(Tp^{Me2})_2(\eta^1\text{-}OC_6H_2(^tBu)_2O)]$, **4**, each of which was structurally characterized. In the case of the less-hindered benzoquinone, an unimetallic semiquinone $[Sm(Tp^{Me2})_2(OC_6H_4O)]$, **5**, could be isolated, although it was unstable with respect to formation of the dimetallic complex $[Sm(Tp^{Me2})_2]_2(\mu\text{-}OC_6H_4O)$, **6**. Compound **6** was structurally characterized, as was its anthraquinone analogue $[Sm(Tp^{Me2})_2]_2(\mu\text{-}OC_{14}H_8O)$, **7**. When the analogous reaction was carried out between the less-reducing $[Eu(Tp^{Me2})_2]$ and benzoquinone, only the europium analogue of the semiquinone **5**, $[Eu(Tp^{Me2})_2(OC_6H_4O)]$, **8**, could be isolated. The use of the sterically hindered 3,5-di-*tert*-butyl-*o*-benzoquinone allowed isolation of $[Sm(Tp^{Me2})_2(DTBSQ)]$, **9**.

## Introduction

Although organic ketyls have been known for more than a century,[1] solid-state structural details on these synthetically useful, but highly reactive, species have only become available thanks to the work of Hou and Wakatsuki.[2] By judicious choice of sterically demanding ligands, these workers showed that alkali metal,[3] alkaline earth,[4a] zirconium,[4b] and lanthanide metal[5] ketyl complexes could be isolated and structurally characterized. One of the more striking features of the chemistry of ketyl species is the observation of pinacol formation, a reaction which has been shown to be strongly dependent on the solvent and on the steric environment of the central metal. In addition, the nature of the isolable ketyl complexes displayed a significant metal dependence. Thus, while all four groups of metals gave crystalline ketyl complexes with fluorenone, only calcium yielded a stable product with the more reactive benzophenone. In contrast, the reaction of benzophenone with the bulky Ln(II) aryloxide, $[Ln(OC_6H_2\text{-}^tBu_2\text{-}2,6\text{-}Me\text{-}4)_2(THF)_3]$ (Ln = Sm, Yb) led to the isolation of Ln(III) complexes containing the diphenylmethoxy, $OCHPh_2$, moiety, formed via unstable ketyl complexes that underwent hydrogen atom abstraction to give the observed product.[5c] The only example of a structurally characterized lanthanide(III)−benzophenone ketyl complex

* To whom correspondence should be addressed. E-mail: a.sella@ucl.ac.uk.
[†] ITN.
[‡] University of Alberta.
[§] University College London.
[||] Loughborough University.
[⊥] University of Kansas.

(1) (a) Bechman, F.; Paul, T. *Justus Liebigs Ann. Chem.* **1891**, *266*, 1. (b) Schlenk, W.; Weichel, T. *Ber. Dtsch. Chem. Ges.* **1911**, *44*, 1182. (c) Schlenk, W.; Thal, A. *Ber. Dtsch. Chem. Ges.* **1913**, *46*, 2480.
(2) Hou, Z.; Wakatsuki, Y. *Chem.—Eur. J.* **1997**, *3*, 1005 and references therein.
(3) Hou, Z.; Fujita, A.; Yamazaki, H.; Wakatsuki, Y. *J. Am. Chem. Soc.* **1996**, *118*, 2503.
(4) (a) Hou, Z.; Jia, X.; Wakatsuki, Y. *Angew. Chem., Int. Ed. Engl.* **1997**, *36*, 1292. (b) Hou, Z.; Fujita, A.; Koizumi, T.; Yamazaki, H.; Wakatsuki, Y. *Organometallics* **1999**, *18*, 1979.
(5) (a) Hou, Z.; Miyano, T.; Yamazaki, H.; Wakatsuki, Y. *J. Am. Chem. Soc.* **1995**, *117*, 4421. (b) Hou, Z.; Fujita, A.; Yamazaki, H.; Wakatsuki, Y. *J. Am. Chem. Soc.* **1996**, *118*, 7843. (c) Hou, Z.; Fujita, A.; Zhang, Y.; Miyano, T.; Yamazaka, H.; Wakatsuki, Y. *J. Am. Chem. Soc.* **1998**, *120*, 754.

10.1021/ic701364k CCC: $37.00 
Published on Web 10/03/2007

**Scheme 1**

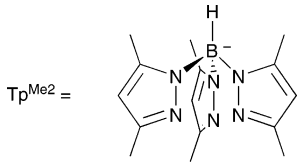


is $[Sm\{C(SiMe_3)_2(SiMe_2OMe)\}_2(OCPh_2)]$, whose structure emphasizes the crucial role played by steric protection in the chemistry of the larger lanthanide ions.[6]

It is now well-established that the hydrotris(pyrazol-l-yl)-borate ligands, $HB(3\text{-}R\text{-}5\text{-}R'pz)_3$, or $Tp^{R,R'}$, with easily tunable steric bulk, are eminently suited for the synthesis of various Ln(II) and Ln(III) complexes.[7] In particular, we have shown that $[Sm(Tp^{Me2})_2]$ (**1**) is a convenient one-electron reductant with the ability to stabilize reactive anionic radical species, such as the azobenzene anion, $[Sm(Tp^{Me2})_2\{N_2(C_6H_5)_2\}]$,[8] and superoxide, $[Sm(Tp^{Me2})_2(\eta^2\text{-}O_2)]$.[9] In this paper we wish to report that **1** reacts with several organic substrates containing C═O groups to yield radical species. Some of them, such as benzophenone, fluorenone, and *p*-$^t$-$Bu_2$benzoquinone, led to isolable radical ketyl complexes that could be characterized crystallographically, while less bulky substrates, such as benzoquinone or anthraquinone, led to bimetallic complexes. The reaction with *o*-$^t Bu_2$benzoquinone gave access to a Sm(III)−semiquinonate complex.

## Results and Discussion

**Reactions with Benzophenone, Fluorenone, and *p*-($^t$Butyl)$_2$benzoquinone**. The addition of stoichiometric amounts of benzophenone, fluorenone, or *p*-$^t Bu_2$benzoquinone to a toluene slurry of $[Sm(Tp^{Me2})_2]$ (**1**) at room-temperature results in immediate dissolution of the purple starting material and formation of deeply colored solutions. Careful workup gives dark-blue $[Sm(Tp^{Me2})_2(\eta^1\text{-}OCPh_2)]$ (**2**), dark-green $[Sm(Tp^{Me2})_2(\eta^1\text{-}OC_{13}H_8)]$ (**3**), and dark-red $[Sm(Tp^{Me2})_2(\eta^1\text{-}OC_6H_2(^tBu)_2O)]$ (**4**) in high yield. The compounds are soluble in common aromatic and ethereal solvents and moderately soluble in aliphatic solvents. The colors of the solutions which, in the absence of oxygen, remain unchanged for

**Scheme 2**

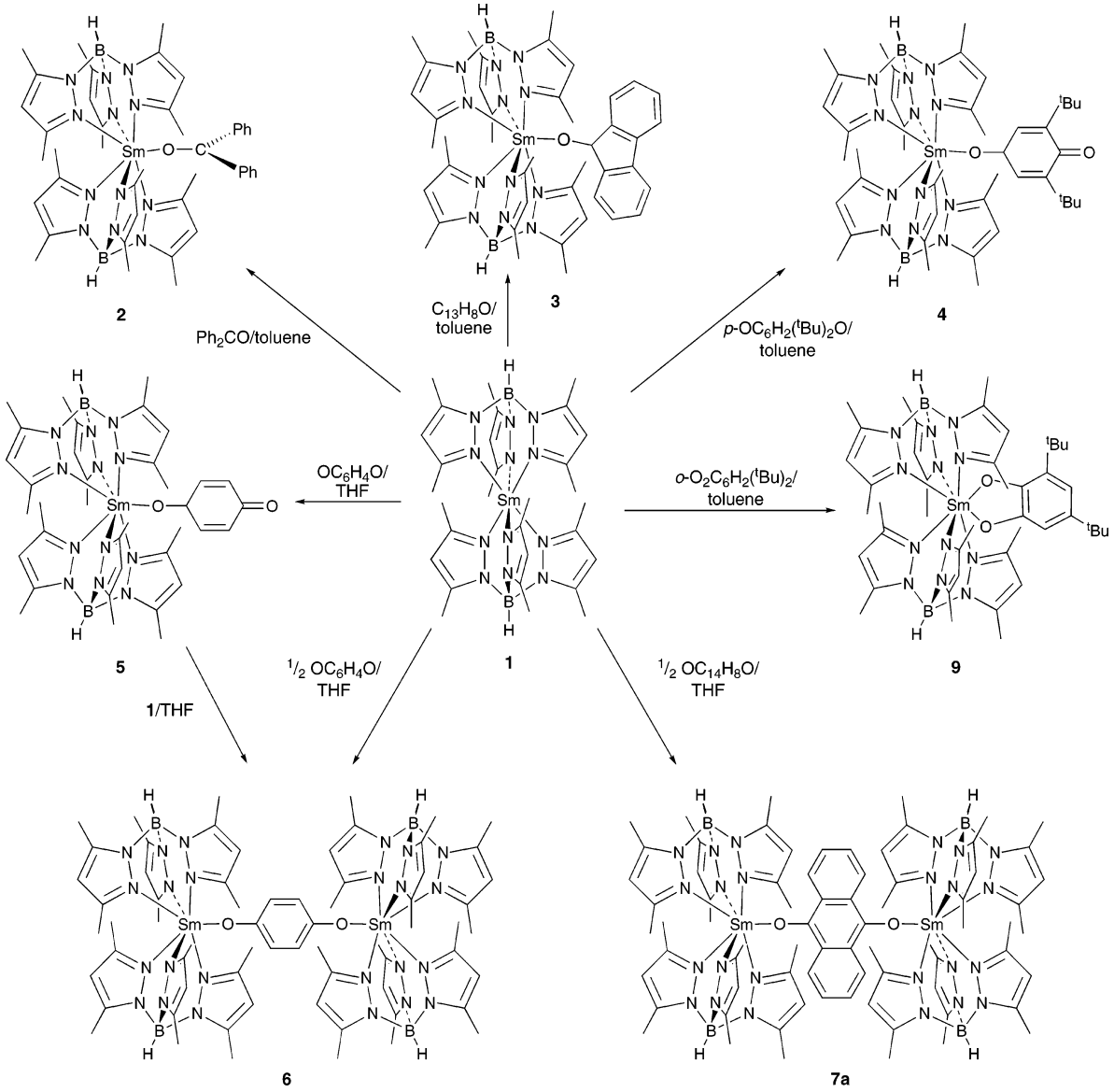

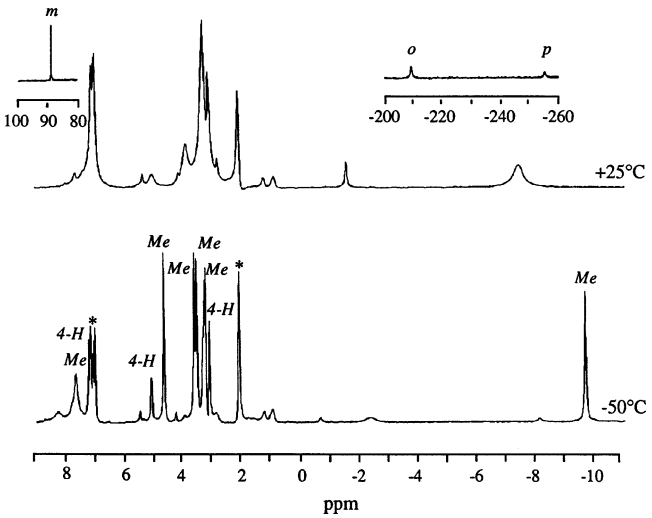


**Figure 1.** Variable-temperature $^1$H NMR spectra of Sm(Tp$^{Me2}$)$_2$(OCPh$_2$), **2**, recorded at +25 (above) and −50 °C (below) in toluene-$d_8$. Asterisk (*) indicates peaks from residual toluene.

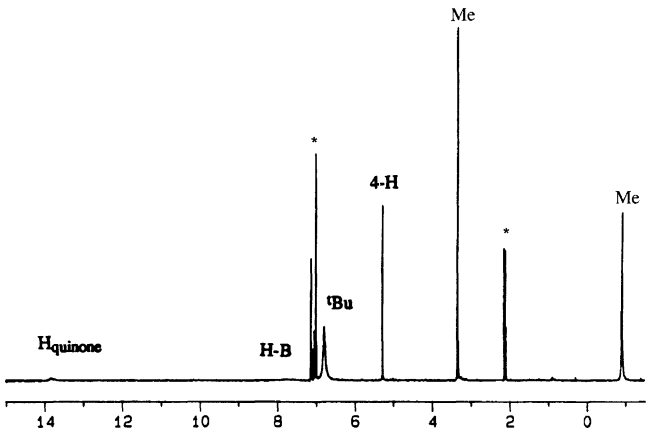


**Figure 2.** $^1$H NMR spectrum of Sm(Tp$^{Me2}$)$_2$(*p*-OC$_6$H$_2$$^t$Bu$_2$O), **4**, recorded at −80 °C in toluene-$d_8$ indicating the fluxional nature of the coordination sphere at this temperature. Asterisk (*) indicates peaks due to residual toluene.

extended periods of time, are typical of ketyl radical anions. The colors are the same in both coordinating and noncoordinating solvents, which is contrary to the observation of Hou and Wakatsuki for their Sm(III)−fluorenone ketyl complex.[5] The bleaching of the color in aliphatic solvents in the latter case was attributed to pinacol formation. Clearly the steric protection afforded by the two Tp$^{Me2}$ ligands is responsible for both the stability of the complex and for the lack of C−C bond formation. In the case of **4**, steric hindrance provided by the two bulky *t*Bu groups prevents approach of a second [Sm(Tp$^{Me2}$)$_2$] molecule and formation of a dimeric compound. A similar observation was made in the reaction of *p*-$^t$Bu$_2$benzoquinone with [Ce(OC$^t$Bu$_3$)$_3$],[10] although in this case, [Ce(OC$^t$Bu$_3$)$_3$($\eta^1$-OC$_6$H$_2$($^t$Bu)$_2$O)] showed signs of decomposition after several hours at room temperature in C$_6$D$_6$.

**$^1$H NMR Studies**. Further evidence for the presence of the radical anions comes from the $^1$H NMR spectra of the complexes. At ambient temperature, the spectrum of **2** (Figure 1) displayed, in addition to the broad, ill-defined signals from the Tp$^{Me2}$ ligands, three highly shifted resonances with a 1:2:2 intensity ratio at −255.2, −209.2, and 88.8 ppm, respectively. The resonance positions are in the same region as those of the phenyl protons in the related complex [Sm(Tp$^{Me2}$)$_2${N$_2$(C$_6$H$_5$)$_2$}],[8] containing the azobenzene radical anion, and are consequently assigned to the phenyl protons of the benzophenone ketyl radical anion. The highest field signal, at −255.2 ppm, can be confidently assigned to the *para* position, on the basis of intensity. Assignment of the remaining resonances rests on the expectation that delocalization of the spin density onto the ring should produce chemical shifts that alternate in direction between adjacent positions.[11] Thus the downfield signal at 88.8 ppm is assigned to the *meta*, while the other high field peak at −209.2 ppm is from the *ortho* protons, respectively. It is interesting to note that in the recently reported benzophenone ketyl complex [Sm{C(SiMe$_3$)$_2$(SiMe$_2$OMe)}$_2$-(OCPh$_2$)}] the $^1$H NMR signals from phenyl group protons could not be detected.[6]

We thought initially that the broad Tp$^{Me2}$ signals at room temperature, especially the feature at 3.3 ppm, resulted from some fluxional process, as has been observed in other Tp$^{Me2}$ systems. However, the $^1$H VTNMR spectra did not support this. As the temperature was lowered, the signals shifted because of the temperature dependence of the magnetic susceptibility[11] and moved apart without decoalescence. At −50 °C, a well-resolved spectrum with six Me and three 4-H pyrazolyl singlets was obtained (Figure 1). The spectrum is consistent with a C$_2$ symmetric structure in which the two Tp$^{Me2}$ ligands are chemically equivalent but the pyrazolyl groups within each are different. The NMR spectrum of **3** was quite similar to that of **2** with four resonances in the ratio 1:1:1:1 at −266.5, −220.5, 89.7, and 6.7 assigned to the protons of the fluorenone anion. At low temperature, the resonances of the Tp$^{Me2}$ ligands were also split into a pattern consistent with a $C_2$-symmetric coordination sphere.

In contrast to the rigid solution structures of compounds **2** and **3**, the less-hindered **4** exhibited a simple $^1$H NMR spectrum (Figure 2), consistent with the molecule undergoing a facile fluxional process that renders all six dimethylpyrazolyl groups of the ancillaries equivalent. It is noteworthy that in the present case the aryl-hydrogens of the coordinated *p*-benzoquinone ligand can be seen as a very broad signal at 14 ppm, whereas in [Ce(OC$^t$Bu$_3$)$_3$($\eta^1$-OC$_6$H$_2$($^t$Bu)$_2$O)], they remain undetected.[10]

**Reactions with 1,4-Benzoquinone and Anthraquinone**. The addition of 1 equiv of 1,4-benzoquinone to a suspension of [Sm(Tp$^{Me2}$)$_2$] in THF solution led to a rapid dissolution

(6) Clegg, W.; Eaborn, C.; Izod, K.; O'Shaughnessy, P.; Smith, J. D. *Angew. Chem., Int. Ed. Engl.* **1997**, *36*, 2815.
(7) (a) Marques, N.; Sella, A.; Takats, J. *Chem. Rev.* **2002**, *102*, 2137−2160. (b) Santos, I.; Marques, N. *New J. Chem.* **1995**, *19*, 55.
(8) Takats, J.; Zhang, X. W.; Day, V. W.; Eberspacher, T. A. *Organometallics* **1993**, *12*, 4286.
(9) Zhang, X. W.; Loppnow, G. R.; McDonald, R.; Takats, J. *J. Am. Chem. Soc.* **1995**, *117*, 7828.
(10) Sen, A.; Stecher, H. A.; Rheingold, A. L. *Inorg. Chem.* **1992**, *31*, 473−479.
(11) Horrocks, W. DeW., Jr.; Eaton, D. R. in LaMar, G. N.; Horrocks, W. De W., Jr.; Holm, R. H. *NMR of Paramagnetic Molecules*; Academic Press: New York, 1973; Chapters 4 and 5.

of the purple starting material, yielding a dark blue solution, from which the blue compound $[Sm(Tp^{Me2})_2(OC_6H_4O)]$ **(5)** was isolated.

Attempts to obtain crystals suitable for X-ray diffraction analysis failed as crystallization of **5** from THF or toluene solutions led always to the formation of yellow crystals of $[Sm(Tp^{Me2})_2]_2(\mu\text{-}OC_6H_4O)$ **(6)**. This behavior is in sharp contrast to the stability of complex **4**. Clearly, the absence of the $^t$Bu groups close to the oxygen of the quinone promotes formation of the dimeric compound. Analogous compounds in which a catecholate group $(OC_6H_4O)^{2-}$ bridges two metal centers have been reported previously. For example, cyclopentadienyl titanium(III) halides and alkyls react with benzoquinone to yield quinone-bridged complexes regardless of the stoichiometric ratios for the reagents.[12] A dimeric compound in which the $(OC_6H_4O)^{2-}$ dianion bridges two cerium centers has been obtained when two molecules of $Ce(OC^tBu_3)_3$ are oxidized by 1,4-benzoquinone.[10] In both cases, it has been suggested that complex formation proceeds stepwise via the initial formation of a semiquinone complex. This has been corroborated in the latter case.[10]

Compound **6** could be easily obtained on a preparative scale by reaction of 2 equiv of $[Sm(Tp^{Me2})_2]$ with the quinone (eq 1) or by reaction of **5** with 1 equiv of $[Sm(Tp^{Me2})_2]$ (eq 2).

$$2[Sm(Tp^{Me2})_2] + OC_6H_4O \rightarrow [Sm(Tp^{Me2})_2]_2(\mu\text{-}OC_6H_4O) \quad (1)$$

$$[Sm(Tp^{Me2})_2(OC_6H_4O)] + [Sm(Tp^{Me2})_2] \rightarrow [Sm(Tp^{Me2})_2]_2(\mu\text{-}OC_6H_4O) \quad (2)$$

In an analogous reaction, an anthraquinone-bridged dimer could be obtained in high yield by reaction in THF at room temperature. The purple $[Sm(Tp^{Me2})_2]$ could be seen to dissolve to give a bright red solution of $[Sm(Tp^{Me2})_2]_2(\mu\text{-}OC_{14}H_8O)$, **7** (eq 3).

$$2[Sm(Tp^{Me2})_2] + OC_{14}H_8O \rightarrow [Sm(Tp^{Me2})_2]_2(\mu\text{-}OC_{14}H_8O) \quad (3)$$

Compound **7** was found to be sparingly soluble in nonpolar hydrocarbons, but dissolved easily in dichloromethane and THF and could be crystallized from $CH_2Cl_2$/toluene at low temperature. Attempts to prepare the 1:1 semiquinone complex with $[Sm(Tp^{Me2})_2]$ were not successful, compound **7** being isolated in each case.

In an attempt to isolate a more stable semiquinone complex, analogous experiments were carried out using the less-reducing Eu(II) complex $[Eu(Tp^{Me2})_2]$. The addition of quinone to a suspension of $[Eu(Tp^{Me2})_2]$ in a 1:1 stoichiometric ratio resulted in the immediate disappearance of the bright orange starting compound and the formation of a deep blue solution. The cobalt blue compound $[Eu(Tp^{Me2})_2(OC_6H_4O)]$ (**8**) was obtained after standard workup (eq 4).

$$[Eu(Tp^{Me2})_2] + OC_6H_4O \rightarrow [Eu(Tp^{Me2})_2(OC_6H_4O)] \quad (4)$$

Formation of the semiquinone complex **8** by transfer of one electron from the $Eu^{2+}$ to the quinone was demonstrated by the Mössbauer spectrum of the compound which at 80 K displayed a single absorption resonance at 0.5 mm $s^{-1}$ characteristic of a $Eu^{3+}$ center.[13]

In contrast with **5**, the addition of a stoichiometric amount of $[Eu(Tp^{Me2})_2]$ to a blue solution of **8** did not lead to a dimeric compound analogous to **6**, the insoluble $[Eu(Tp^{Me2})_2]$ being recovered unchanged from the reaction mixture. Clearly, the reducing power of $[Eu(Tp^{Me2})_2]$ is enough to reduce the quinone to the semiquinone stage (the potential associated with the first reduction process is not strictly known but it is likely to be $\sim$0.30 V)[14] but not to reduce the semiquinone to its catecholate form. Although **8** is stable in solution, attempts to obtain crystals of this compound were unsuccessful because **8** precipitated as a blue powder from THF or toluene solutions.

**$^1$H NMR Studies**. The room temperature $^1$H NMR spectra of **5** and **6** display three single peaks in the ratio 3:3:1 assigned to the tris(pyrazolyl)borate ligands. The deceptively simple spectra are indicative of fluxional behavior, as observed in other pyrazolyl groups of seven-coordinate $[Sm(Tp^{Me2})_2X]$ compounds.[15] In addition, the $^1$H NMR spectrum of **5** showed one resonance at 10.39 ppm assigned to two protons of the quinone and a very broad resonance at 7.6 ppm, which integrated for the remaining two protons of the quinone and for the two protons of the B−H groups. In the spectrum of **6**, a single resonance at 12.6 ppm was assigned to the four equivalent protons of the quinone, and one broad resonance at 8.0 ppm integrated for the four protons of the B−H groups.

Variable-temperature NMR studies were undertaken. When **5** and **6** were cooled in toluene-$d_8$, the resonances shifted because of the temperature dependence of the magnetic susceptibility and broadened, but limiting spectra could not be reached in toluene solution.

The $^1$H NMR spectrum of **7** was consistent with a nonfluxional molecule of $C_2$-symmetry around the metal, giving a total of 11 peaks, arising from the six independent methyl groups, three pyrazolyl 4-CH groups, and two aromatic hydrogens. The spectra were temperature invariant between +20 and 80 °C. Although the more soluble analogue, $[Sm(Tp^{Me2\text{-}4\text{-}Et})_2]_2(\mu\text{-}OC_{14}H_8O)$, **7b**, could be prepared analogously, we were unable to isolate it in analytically pure form.

(12) Künzel, A.; Sokolow, M.; Liu, F.; Roesky, H. W.; Noltemeyer, M.; Schmidt, H.; Usón, I. *J. Chem. Soc., Dalton Trans.* **1996**, 913−919.

(13) Grandjean F.; Long G. J. In *Mössbauer Spectroscopy Applied to Inorganic Chemistry*; Long, G. J., Grandjean, F., Eds.; Plenum Press: New York, 1989; Vol. 3, pp. 513−597.

(14) Connelly, N. G.; Geiger, W. E. *Chem. Rev.* **1996**, *96*, 877−910.

(15) (a) Hillier, A. C.; Liu, S.; Sella, A.; Elsegood, M. R. J. *Inorg. Chem.* **2000**, *35*, 2635−2644. (b) Hillier, A. C.; Zhang, X. W.; Maunder, G. H.; Liu, S. Y.; Eberspacher, M. V.; McDonald, R.; Domingos, A.; Marques, N.; Day, V. W.; Sella, A.; Takats, J. *Inorg. Chem.*, **2001**, *40*, 5106−5116. (c) Lopes, I.; Monteiro, B.; Lin, G.; Domingos, Â.; Marques, N.; Takats, J. *J. Organomet. Chem.* **2001**, *632*, 119−125.

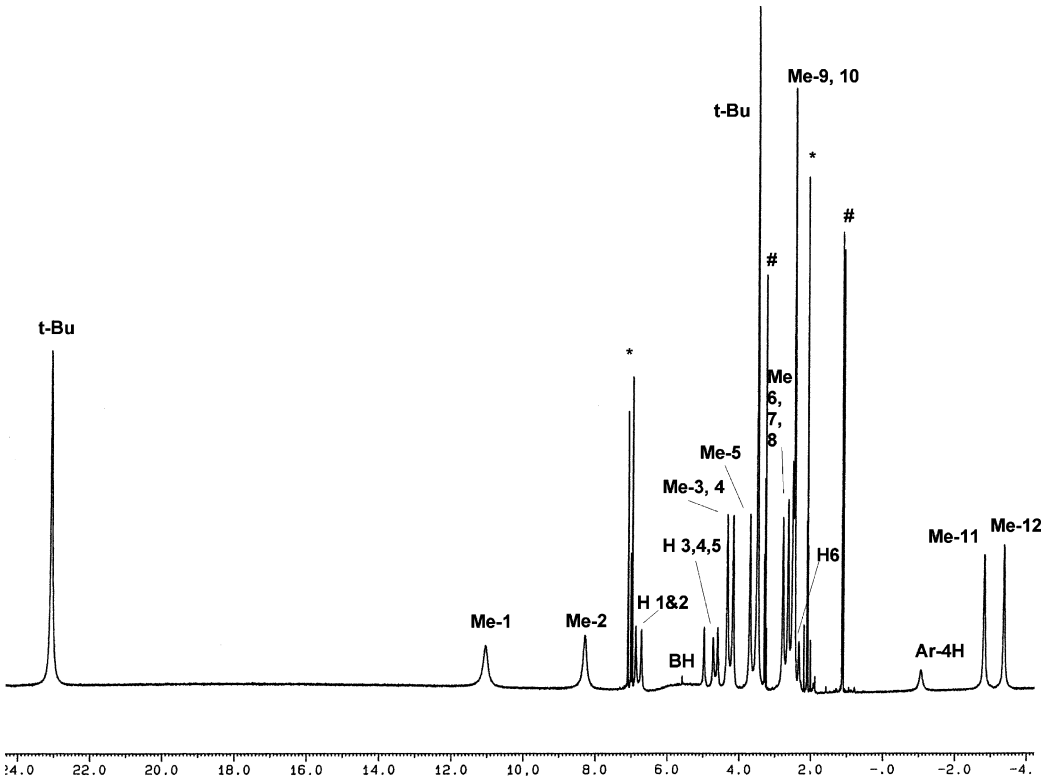


**Figure 3.** Room-temperature $^1$H NMR spectrum of Sm(Tp$^{Me2}$)$_2$(DTBSQ), **9**, in toluene-$d_8$ consistent with a stereochemically rigid coordination sphere. Asterisk (*) indicates peaks due to residual toluene. # indicates peaks due to diethyl ether.

The NMR spectra were, however, consistent with the proposed formulation.

The room-temperature $^1$H NMR spectrum of **8** displays one set of resonances in the ratio 3:3:1 assigned to the Tp$^{Me2}$ ligands, but the resonances from the protons of the quinone could not be found, even at low temperature.

**Reaction with 3,5-Di-*tert*-butyl-*o*-benzoquinone (DTBQ).** Although a bis-Tp supported Gd(III) semiquinonate complex is known, [GdTp$_2$(DTBSQ)], (DTBSQ = 3,5-di-*tert*-butyl-*o*-semibenzoquinonate),[16] it was of interest to see if a similar complex obtained by the reaction of [Sm(Tp$^{Me2}$)$_2$] (**1**) with DTBQ because, as expected, the gadolinium(III) complex was formed under rather different conditions. Indeed, the addition of 1 equiv of DTBQ to a slurry of [Sm(Tp$^{Me2}$)$_2$] in THF at room temperature (RT) resulted in a rapid dissolution of the purple starting material and formation of a deep green solution from which green crystalline [Sm(Tp$^{Me2}$)$_2$(DTBSQ)] (**9**) was isolated in good yield by standard workup.

The $^1$H NMR spectrum of **9** at room temperature, Figure 3, was indicative of a rigid structure in solution but with some overlapping Tp−Me signals. A broad signal at −1.25 ppm was assigned to the shifted *m*-ArH proton of the DTBSQ ligand. On the other hand, we could not locate the peak associated with the *o*-ArH, which we expected to be broader and more strongly shifted because of its proximity to the metal. Lowering the temperature resolved the overlapping Tp−Me signals but failed to reveal the position of the *o*-ArH resonance. At −80 °C, the $^1$H NMR spectrum is consistent with a $C_1$-symmetric structure, with 12 Tp−Me, 6 pyrazolyl 4-CH, and 2 DTBSQ $^t$Bu signals. The broad peak at −8.80 ppm is assigned to the *m*-ArH, which shifts sharply from its room-temperature position because of the temperature dependence of the magnetic susceptibility.

**X-ray Crystallography.** Solid-state structures, determined by single-crystal X-ray diffraction, confirmed the identity, established the precise coordination geometry and provided metrical parameters for complexes **2**−**4**, **6**, **7**, and **9**.

ORTEP views of molecules **2**−**4** are shown in Figures 4−6, respectively. Selected bond distances and angles are listed in Table 1. Each samarium center is seven-coordinate with two tridentate Tp$^{Me2}$ ligands staggered with respect to each other and the benzophenone, fluorenone, or *p*-$^t$Bu$_2$-quinone oxygen occupying the seventh site. The coordination geometry, which is necessarily distorted because of the constrained nature of the tridentate Tp$^{Me2}$ ligands, could in all cases be described as distorted pentagonal bipyramidal. Reference to the figures shows that, although the solid-state structures have $C_1$-symmetry, small angle deformations coupled with oscillation of the ketone moiety between the pyrazolyl groups anchored by N(2) and N(4) in **2** and N(1) and N(4) in **3** will give species with time-averaged $C_2$ molecular symmetry, in accord with the solution NMR behavior of the complexes.

The average pyrazolyl Sm−N distances (2.56(6) Å in **2**, 2.56(4) Å in **3**, and 2.55(6) Å in **4**) compare well with the 2.59(6) and 2.58(7) Å averages observed for these bonds in [Sm(Tp$^{Me2}$)$_2${N$_2$(C$_6$H$_5$)$_2$}][7] and [Sm(Tp$^{Me2}$)$_2$($\eta^2$-O$_2$)][8] , respectively. The Sm−O(1) distances of 2.201(3) Å in **2**,

(16) Caneschi, A.; Dei, A.; Gatteschi, D.; Sorace, L.; Vostrikova, K. *Angew. Chem., Int. Ed.* **2000**, *39*, 246.

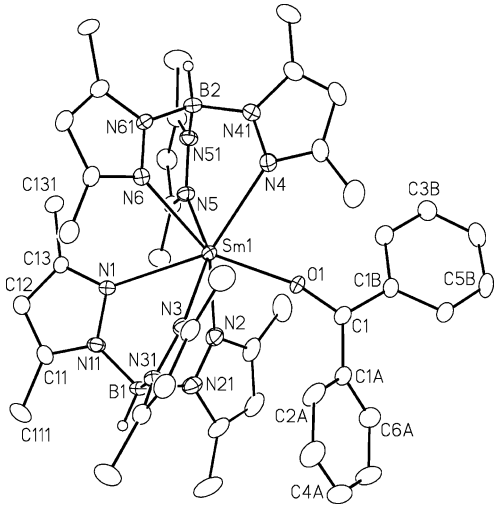


**Figure 4.** Molecular structure of $Sm(Tp^{Me2})_2(OCPh_2)$, **2**, with the non-hydrogen atoms represented at the 50% probability level.

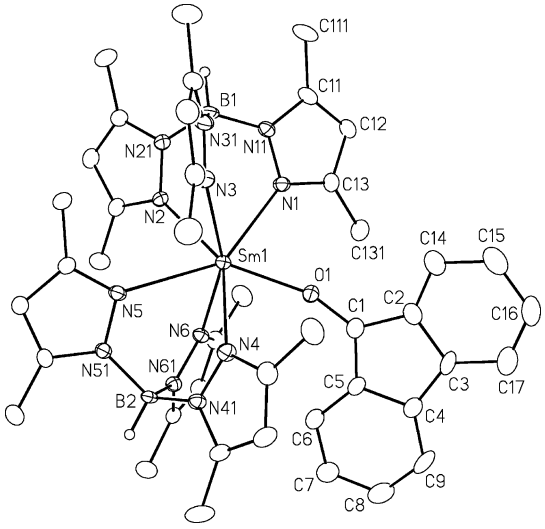


**Figure 5.** Perspective view of $Sm(Tp^{Me2})_2(OC_{13}H_8)$, **3**, with the non-hydrogen atoms represented at the 50% probability level.

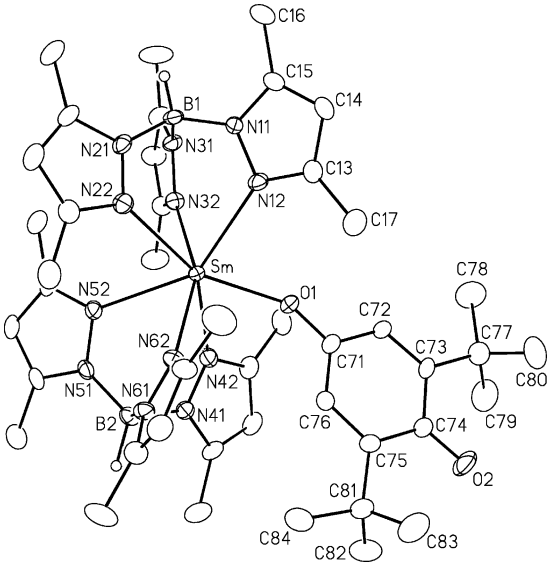


**Figure 6.** Molecular structure of $[Sm(Tp^{Me2})_2(\eta^1\text{-}OC_6H_2(^tBu)_2O)]$, **4**, with the non-hydrogen atoms represented at the 50% probability level.

2.186(4) Å in **3**, and 2.208(5) Å in **4** are all somewhat longer than the corresponding Sm−O distances in other structurally characterized Sm(III) complexes: 2.13(1) Å in (formally 7-coordinate) $[Cp^*_2Sm(OC_6Me_4H)]$,[17] 2.143(5) Å in 5-coordinate $[Sm(OAr)(OCHPh_2)_2(HMPA)_2]$,[18] and 2.093(3) Å in the 5-coordinate samarium benzophenone ketyl complex, $[Sm\{C(SiMe_3)_2(SiMe_2OMe)\}_2(OCPh_2)]$.[6] These differences reflect the higher coordination numbers or the more sterically demanding nature of the tridentate ligands bound to the samarium center in the pyrazolylborate complexes. These Sm−O bond lengths do follow the expected trend of being shorter than those in Sm(II)−aryloxides, such as $[Sm(OAr)_2(THF)_3]$ (av 2.304(8) Å).[19] Final corroboration for the formulation of **2** as a Sm(III) ketyl comes from the distances and geometry of the radical moiety. The lengths of the coordinated O(1)−C(1) bonds (1.322(6) Å in **2**, 1.305(7) Å in **3**, and 1.305(9) Å in **4)** are significantly longer than that of free benzophenone (1.23(1) Å)[20] and that of the free C(2)−O(2) double bond in **4** (1.262(10) Å).These coordinated C−O bond lengths compare well with the values reported by Hou and Wakatsuki for the calcium−benzophenone ketyl (av 1.31(2) Å)[4] and the fluorenone ketyl (1.27−1.31 Å)[5] complexes. They are also slightly shorter than the 1.346(6) Å Sm−O bond in $[Sm\{C(SiMe_3)_2(SiMe_2OMe)\}_2(OCPh_2)]$.[5] Because the geometry of the carbon atom for each of these coordinated carbonyls is planar within experimental error, these carbons remain $sp^2$-hybridized.

Compound **6**, $[Sm(Tp^{Me2})_2]_2(\mu\text{-}OC_6H_4O)$, crystallized from a toluene solution in the space group $P\bar{1}$ with two-half molecules of toluene included in the lattice. The asymmetric unit is composed of two separate half molecules related by an inversion center. An ORTEP view of the molecule is shown in Figure 7, and selected bond lengths and angles are given in Table 1. Each samarium center is seven-coordinate by the two tridentate Tp ligands staggered with respect to each other and one oxygen atom of the quinone occupying the seventh site. The coordination geometry is best described as a distorted pentagonal bipyramid with N(12) and N(52) occupying the axial sites (N(12)−Sm−N(52) = 154.8(3)°) and N(22), N(32), N(42), N(62), and O(1) occupying the equatorial positions for Sm(1). For Sm(2), the N(12A) and N(52A) occupy the axial sites (N(12A)−Sm(2)−N(52A) = 153.5(3)°), while N(22A), N(32A), N(42A), N(62A), and O(2) span the equatorial positions. The average Sm−N distance (2.57(6) Å) is comparable to the values of 2.572(5) Å in $[Sm(Tp^{Me2})_2(OPh\text{-}4\text{-}Bu^t)]$,[15a] 2.58(3) Å in $[Sm(Tp^{Me2})_2F]$, and 2.56(4) Å in $[Sm(Tp^{Me2})_2Cl]$.[15b] The Sm−O distances of 2.136(8) and 2.110(9) Å are slightly shorter than those observed in the seven-coordinate $[Sm(Tp^{Me2})_2(OPh\text{-}4\text{-}Bu^t)]$ (2.159(2) Å)[15a] and $[Sm(Tp^{Me2})_2(OPh\text{-}2,4,6\text{-}Bu^t)]$ (2.188 (5) Å). [15c.] The C−O bond distances of 1.356(15) and 1.369(15) Å are similar to those observed in $[Ce(OC^t$-

(17) Evans, W. J.; Hanusa, T. P.; Levan, K. R. *Inorg. Chim. Acta* **1985**, *110*, 191.
(18) Hou, Z.; Yoshimura, T.; Wakatsuki, Y. *J. Am. Chem. Soc*. **1994**, *116*, 11169.
(19) Qi, G. Z.; Shen, Q.; Lin, Y. H. *Acta Crystallogr., Sect. C* **1994**, *50*, 1456.
(20) Fleischer, E. B.; Sung, N.; Hawkinson, S. *J. Phys. Chem.* **1968**, *72*, 4311.

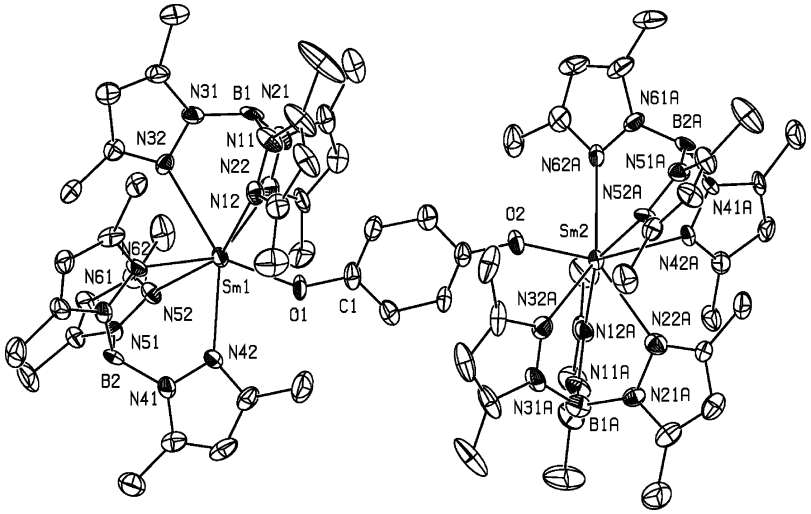


**Figure 7.** Perspective view of $[Sm(Tp^{Me2})_2]_2(\mu\text{-}O_2C_6H_4)$, **6**, with non-hydrogen atoms represented at the 50% probability level.

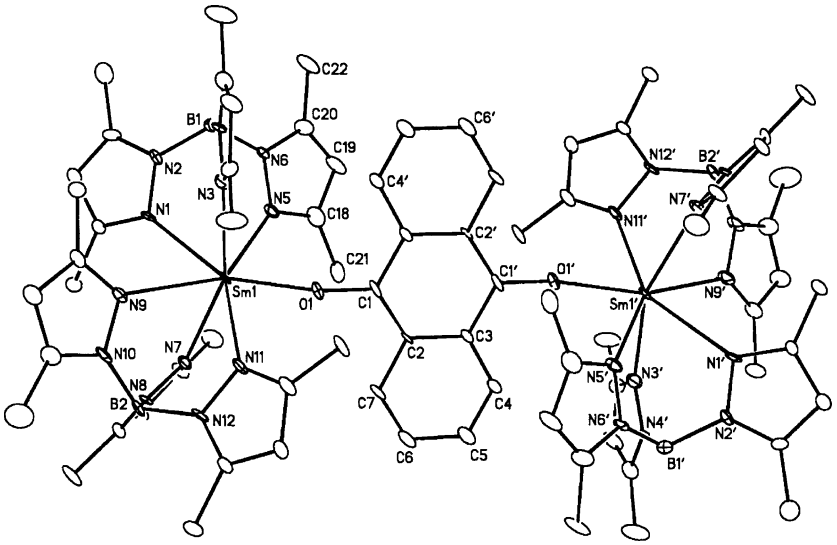


**Figure 8.** Perspective view of $[Sm(Tp^{Me2})_2]_2(\mu\text{-}O_2C_{14}H_8)$, **7**, with non-hydrogen atoms represented at the 50% probability level.

**Table 1.** Selected Bond Lengths (Å) and Angles (deg) for **2**·0.5$C_6H_8$, **3**·$C_7H_8$, **4**, **6**·$C_7H_8$, **7**·2$CH_2Cl_2$, and **9**·0.5$C_7H_8$

| | **2**·0.5$C_6H_8$ | **3**·$C_7H_8$ | **4**·$C_7H_8$ | **6**·$C_7H_8$ | **7**·$CH_2Cl_2$ | **9** |
|---|---|---|---|---|---|---|
| av(Sm−N) | 2.56(6) | 2.56(4) | 2.55(6) | 2.57(6) | 2.572(4) | 2.58(6) |
| Sm−$O_1$ | 2.200(3) | 2.186(4) | 2.208(5) | 2.136(8) | 2.138(8) | 2.428(4) |
| Sm-$O_2$ | | | | 2.110(8) | | 2.386(3) |
| C−$O_1$ | 1.322(6) | 1.305(7) | 1.305(9) | 1.356(14) | 1.326(14) | 1.278(5) |
| C−$O_2$ | | | 1.262(10) | 1.369(14) | | 1.284(5) |
| ∠Sm−$O_1$−$C_1$ | 160.8(3) | 161.7(4) | 154.2(6) | 147.9(9) | 167.5(8) | |
| ∠Sm−$O_2$−$C_2$ | | | | 153.7(8) | | |
| ∠B(1)−Sm−B(2) | 145.7(1) | 146.0(2) | 146.3(2) | 144.5(4) | 143.1(9) | 149.4(1) |
| ∠B(1A)−Sm−B(2A) | | | | 147.6(4) | | |

$Bu_3)_3]_2(\mu\text{-}OC_6H_4O)$ (1.375(15) Å)[10] and $[Ti(Cp^*)_2Cl]_2(\mu\text{-}OC_6H_4O)$ (1.352(3) Å)[12] and longer than those in the radical anionic species **2**, **3**, and **4** (vide supra). The carbonyl carbon atoms of the ketones are in $sp^2$-hybrid states, as can be seen in the sum of the angles around C(1) and C(2), which is close to 360°.

X-ray quality crystals of **7** were grown from dichloromethane/THF solution as red plates in space group $P\bar{1}$. The molecular structure is shown in Figure 8. No significant intermolecular contacts were noted. Like compound **6**, compound **7** consists of an anthraquinone-bridged dimer. The metal coordination sphere is typical of these seven-coordinate systems and merits little comment. Two of the pyrazolyl rings twist about the B−N bond by 22.0 and 23.7°, respectively, as a result of distortions necessary to accommodate the anthraquinone group, but there is no evidence for interaction of the pyrazolyls with the aromatic rings of the bridge.

The Sm−O bond in **7**, 2.138(8) Å, is similar to that in the quinone, **6**, but shorter than those in the corresponding phenoxides (vide infra) suggesting that the negative charge is more localized on the donor oxygen in these systems. On the other hand, the Sm−O bond is slightly longer than those observed in the related metallocene systems $[Cp^*_2Sm(O\text{-}2,3,5,6\text{-}Me_4C_6H)]$[17] 2.13(1) Å, $[Cp^*_2Sm]_2(O_2C_{16}H_{10})$ 2.08(2)

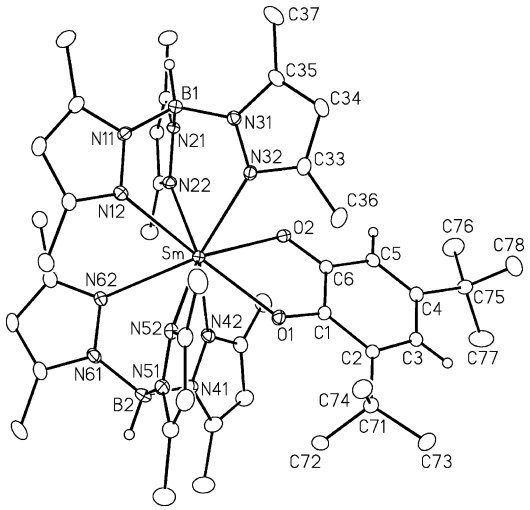


**Figure 9.** Molecular structure of [Sm(Tp$^{Me2}$)$_2$(DTBSQ)], **9**, with non-hydrogen atoms represented at the 50% probability level.

Å, and [Cp*$_2$Sm]$_2$($O_2C_{16}H_{10}$) 2.099(9) Å,[21] reflecting the greater crowding around the third ligand in the Tp$^{Me2}$ system than in the relatively open wedge of the metallocene. The Sm−O−C angle of 167.6(8)°, which approaches linearity, is larger than in the other complexes described in this study and simply reflects the lateral extension of the anthraquinone, which therefore prevents bending.

The sum of the angles around the bridgehead carbon C(1) indicate that it is planar, suggesting that it is still sp$^2$-hybridized and that compound **7** is a quinone dianion metal complex, consistent with the fact that it is formed via an electron-transfer route. The C(1)−O(1) bond length of 1.326-(14) Å is typical of metal alkoxide systems.[22]

The molecular structure of **9** is shown in Figure 9, and selected bond distances and angles are listed in Table 1. The Sm center is eight-coordinate by six nitrogen atoms from the two staggered tridentate Tp$^{Me2}$ ligands and two oxygen atoms of the DTBSQ ligand. The coordination geometry, like that of the analogous [GdTp$_2$(DTBSQ)] complex, is best described as distorted square-antiprism with O(1),N(32),N-(12),N(52) and O(2),N(22),N(62),N(42) describing the approximate square faces. The average Sm−N and Sm−O bond distances (2.58(6) and 2.41(1) Å) are somewhat longer than those in the Gd complex (2.53(5) and 2.35(1) Å), reflecting the larger size of the Tp$^{Me2}$ ligand and consequently more congested environment of Sm in complex **9**. The increase in these distances is larger than expected from the larger size of the Sm center.[23] The average C−O and C(1)−C(6) bond lengths (1.281(5) and 1.452(6) Å) are slightly longer/shorter than the corresponding distances in the Nd analogue (1.26 (2) and 1.49(2) Å) and are in the range expected in semiquinone complexes (1.29 and 1.44 Å).[24]

## Conclusions

This study further demonstrates the ability of the [Sm-(Tp$^{Me2}$)$_2$] fragment to trap anionic organic radicals. It is the fortuitous coincidence of steric protection provided by the two Tp$^{Me2}$ ligands and the size of the substrate which prevents the pinacol formation by C−C coupling, which has been observed with samarium−fluorenone ketyl complexes, and is responsible for the solution rigid structures of the complexes. Less-hindered substrates result in formation of dimeric compounds.

## Experimental Section

All preparations and subsequent manipulations were carried out using standard Schlenk line and glovebox techniques in an atmosphere of dinitrogen. THF, toluene, and *n*-hexane were dried by standard methods and degassed before use. Deuteriated solvents, benzene-$d_6$ and toluene-$d_8$, were dried over Na and distilled. Benzoquinone was repeatedly sublimed before use. Ln(Tp$^{Me2}$)$_2$ (Ln = Sm, Eu) and [Sm(Tp$^{Me2-4-Et}$)$_2$] were prepared according to the literature procedures.[15b] $^1$H NMR spectra were recorded on Varian VXR 300 or Bruker AMX400 spectrometers and referenced internally using the residual solvent resonances relative to tetramethylsilane. IR spectra were recorded as Nujol mulls or KBr pellets on a Perkin-Elmer 2000-FT-IR spectrometer. Carbon, hydrogen, and nitrogen combustion analyses were performed in-house using Perkin-Elmer automatic analyzers.

Transmission Mössbauer spectra were measured in the velocity range of ±30 mm s$^{-1}$ at room temperature and 80 K using a liquid nitrogen flow cryostat. Experimental details are as described previously.[25] The isomer shifts are given relative to the $^{151}SmF_3$ source at room temperature. At room temperature, only a small absorption ~0 mm s$^{-1}$ was observed, but the quality of the spectrum was very poor suggesting a very low recoilless fraction. At 80 K a well-defined spectrum was obtained. The spectrum was fitted by a single Lorentzian using a nonlinear least-squares method. The estimated isomer shift, 0.50(5) mm s$^{-1}$ relative to the $^{151}SmF_3$ source, is typical of Eu(III);[25] the estimated line width was 3.8(1) mm s$^{-1}$, and no attempts were made to fit a quadrupole splitting because we were only interested in checking the oxidation state of Eu. Because no other peaks are observed in the velocity range of ±30 mm s$^{-1}$ it was concluded that all the Eu in the sample is in the trivalent state.

**[Sm(Tp$^{Me2}$)$_2$(OCPh$_2$)], 2.** A solution of benzophenone (50 mg, 0.274 mmol) in 5 mL of toluene was added dropwise to a slurry of [Sm(Tp$^{Me2}$)$_2$] (204 mg, 0.274 mmol) in 5 mL of toluene. The addition was accompanied by the immediate formation of an ink blue color. After the mixture was stirred for 2 h, the solvent was removed under reduced pressure, and the dark blue solid was washed with a small volume of hexane, with some loss of the compound which is moderately soluble in hexane. The solid was then dried in vacuum (205 mg, 75%). Anal. Calcd for $C_{43}H_{54}N_{12}B_2$-OSm: C, 55.74; H, 5.83; N, 18.14. Found: C, 56.22; H, 5.75; N, 17.63. IR (Nujol, cm$^{-1}$): 2560, 2518 ($\nu_{B-H}$). $^1$H NMR (toluene-$d_8$, −50 °C): $\delta$ 115.5 (4H, H-*m* (OCPh$_2$))), 7.65 (s, 6H, Me), 7.21 (s, 2H, 4-CH), 5.06(s, 2H, 4-CH), 4.65 (s, 6H, Me), 3.60 (s, 6H, Me), 3.53 (s, 6H, Me), 3.23 (s, 6H, Me), 3.10(s, 2H, 4-CH), −9.86 (s, 6H, Me), −241,4 (4H, H-*o* (OCPh$_2$)), −280.7 (2H, H-*p* (OCPh$_2$)). UV−vis (toluene, 25 °C, 3.46 × 10$^{-5}$ M): 343 ($\epsilon$ = 8.6 × 10$^3$ M$^{-1}$ cm$^{-1}$), 588 nm ($\epsilon$ = 1.9 × 10$^3$ M$^{-1}$ cm$^{-1}$).

(21) Evans, W. J.; Hanusa, T. P.; Levan, K. R., *Inorg. Chim. Acta* **1985**, 110, 191−195.
(22) Bradley, D. C.; Mehrotra, R. C.; Rothwell, I. P.; Singh, A. *Alkoxo and Aryloxo Derivatives of Metals*; Academic Press: London, 2001.
(23) Shannon, R. D. *Acta Crystallogr., Sect. A* **1976**, *32*, 751.
(24) (a) Pierpont, C. G.; Buchanan, R. M. *Coord. Chem. Rev.* **1981**, *38*, 45. (b) Pierpont, C. G.; Lange, C. W. *Prog. Inorg. Chem.* **1994**, *41*, 331. (c) Carugo, O.; Castellini, C. B.; Djinovic, K.; Rizzi, M. *J. Chem. Soc., Dalton Trans.* **1992**, 837.
(25) Carretas, J. M.; Branco, J.: Marçalo, J.; Waerenborgh, J. C.; Marques, N.; Pires de Matos, A. *J. Alloys Compds.* **1998**, *277*, 841.

**[Sm(Tp$^{Me2}$)$_2$(OC$_{13}$H$_8$)], 3.** The complex was synthesized as described for **2** by the addition of a solution of fluorenone (36 mg, 0.20 mmol) in toluene to 150 mg (0.20 mmol) of [Sm(Tp$^{Me2}$)$_2$] in toluene to give **3** as a green solid (130 mg, 70%). Anal. Calcd for $C_{43}H_{52}N_{12}B_2OSm$: C, 55.84; H, 5.67; N, 18.17. Found: C, 55.55; H, 5.50; N, 17.31. IR (Nujol, cm$^{-1}$): 2550, 2520 (sh) ($\nu_{B-H}$). $^1$H NMR (toluene-$d_8$, −40 °C): $\delta$ 89.7 (2H, (OC$_{13}$H$_8$)), 73.2 (2H, (OC$_{13}$H$_8$)), 6.72 (s, 2H, 4-CH), 5.13 (s, 6H, Me), 4.98 (s, 6H, Me), 4.62 (s, 2H, 4-CH), 3.76 (s, 2H, 4-CH), 3.41 (s, 6H, Me), 3.30 (s, 6H, Me), 2.41 (s, 6H, Me), −9.03 (s, 6H, Me), −220.5 (2H, (OC$_{13}$H$_8$)), −266.6 (2H, (OC$_{13}$H$_8$)).

**[Sm(Tp$^{Mc2}$)$_2$(OC$_6$H$_2$($^t$Bu)$_2$O], 4.** A solution of 2,6-di-*tert*-butyl-1,4-benzoquinone (205 mg, 0.930 mmol) in ∼3 mL of toluene was added dropwise to a slurry of [Sm(Tp$^{Me2}$)$_2$] (692 mg, 0.930 mmol) in ∼5 mL of toluene. Solid **1** slowly dissolved, and a red solution was obtained at the end of the addition. After the solution was stirred for 4 h, the toluene was removed under vacuum. The residue was washed with ∼3 mL of hexane, and then it was dissolved in ∼3 mL of a mixture of toluene/hexane (2:1). Cooling of the solution at −40 °C for 2 days gave red crystals of **9** (550 mg, 0.570 mmol, 62%). Anal. Calcd for $C_{51}H_{72}N_{12}O_2B_2Sm$: C, 57.94; H, 6.86; N, 15.90. Found: C, 57.73; H, 6.91; N, 15.88. IR (KBr, cm$^{-1}$): 2548 ($\nu_{B-H}$). MS (EI, 70 eV, 220 °C): 744 (M − C$_{14}$H$_{20}$O$_2$)$^+$. $^1$HNMR (toluene-$d_8$, 25 °C): $\delta$ 13.80 (s, 2H, quinone), 7.7 (br. s, 2H, B−H), 6.77 (s, 18H, quinone), 5.26 (s, 6H, pz-H), 3.33 (s, 18H, pz-Me), −0.92 (s, 18H, pz-Me). $^{11}$B NMR (toluene-$d_8$, 25 °C): $\delta$ −1.3 (s).

**[Sm(Tp$^{Me2}$)$_2$(OC$_6$H$_4$O)], 5.** 1,4-Benzoquinone (16 mg, 0.15 mmol) dissolved in THF (5 mL) was slowly added to a slurry of [Sm(Tp$^{Me2}$)$_2$] (113 mg, 0.15 mmol) in 5 mL of THF. After the addition, there is immediate formation of a blue solution. Stirring was continued overnight. Removal of the solvent under reduced pressure yielded a dark blue solid, which was further washed with *n*-hexane and dried under vacuum. Yield: 60% (80 mg, 0.09 mmol). Anal. Calcd for $C_{36}H_{48}N_{12}B_2O_2Sm$: C, 50.70; H, 5.67; N, 19.71. Found: C, 48.73; H, 5.67; N, 19.21. IR (Nujol, cm$^{-1}$): 2555, 2519 (sh) ($\nu_{B-H}$). $^1$H NMR (toluene-$d_8$, 20 °C): $\delta$ 10.4 (2H, br, quinone), 7.7 (4H, br), 5.42 (6H, H-4), 3.19 (18H, Me-5), −1.71 (18H, Me-3).

**[Sm(Tp$^{Me2}$)$_2$]$_2$($\mu$-OC$_6$H$_4$O), 6.** The addition of 1,4-benzoquinone (16 mg, 0.15 mmol) to a slurry of [Sm(Tp$^{Me2}$)$_2$] (220 mg, 0.30 mmol) in THF resulted in the immediate disappearance of the purple color to give a yellow solution. Removal of the solvent under reduced pressure yielded a yellow solid, which was further washed with *n*-hexane and dried under vacuum. Yield: 67% (160 mg, 0.10 mmol). Anal. Calcd for $C_{66}H_{92}N_{24}B_4O_2Sm_2$: C, 49.62; H, 5.80; N, 21.04. Found: C, 47.70; H, 5.84; N, 19.56. IR (Nujol, cm$^{-1}$): 2555, 2519 (sh) ($\nu_{B-H}$). $^1$H NMR (toluene-$d_8$, 20 °C): $\delta$ 12.62 (4H, br), 7.96 (4H, br, B−H), 5.59 (12H, H-4), 3.34 (36H, Me-5), −1.45 (36H, Me-3); (−80 °C) 13.81 (4H, quinone), 8.8 (4H, vbr, B−H), 5.71(12H, H-4), 3.59 (36H, Me-5).

**Preparation of [{Sm(Tp$^{Me2}$)$_2$}$_2$O$_2$C$_{14}$H$_8$], 7a.** [Sm(Tp$^{Me2}$)$_2$], **1**, (100 mg, 0.13 mmol) and 9,10-anthraquinone (13 mg, 0.06 mmol) were mixed in a Schlenk tube under $N_2$, and THF (30 mL) was added at −78 °C. The purple [Sm(Tp$^{Me2}$)$_2$] was dissolved, and the mixture turned deep red over 15 min. The solution was stirred for 2 h as it warmed to room temperature, and then it was filtered. The volume of the filtrate was reduced slightly, and ∼10 mL of $Et_2O$ added. Slow cooling to −30 °C gave 100 mg (0.058 mmol, 88%) of fine red crystals. The product was soluble in THF and $CH_2Cl_2$, sparingly soluble in toluene, $Et_2O$, DME, and petrol, and could also be crystallized at low temperature from a mixture of $CH_2Cl_2$ and toluene.

Anal. Calcd for $C_{74}H_{96}N_{24}B_4O_2Sm_2$: C, 52.35; H, 5.70; N, 19.80. Found: C, 51.11; H, 5.61; N, 18.94. IR (KBr, cm$^{-1}$): 2552, 2525 (BH), 1561−1684 (br) (CO and overtones from anthraquinone). $^1$H NMR ($C_6D_6$): $\delta$ −8.35 (s, 6H, 3-Me), 0.80 (s, 6H, 3(5)-Me), 2.06 (s, 6H, 3(5)-Me), 2.30 (s, 6H, 5(3)-Me), 3.03 (s, 6H, 5(3)-Me), 3.06 (m, 4H, C$_{14}$H$_8$O$_2$), 3.34 (m, 4H, C$_{14}$H$_8$O$_2$), 3.4 (s, 6H, 5(3)-Me), 5.57 (s, 2H, 4-CH), 5.79 (s, 2H, 4-CH), 6.00 (s, 2H, 4-CH).

**Preparation of [{Sm(Tp$^{Me2\text{-}4\text{-}Et}$)$_2$}$_2$O$_2$C$_{14}$H$_8$], 7b.** The reaction was carried out analogously to the preparation of **4a**, using 100 mg (0.11 mmol) of [Sm(Tp$^{Me2\text{-}4\text{-}Et}$)$_2$] and 11 mg (0.05 mmol) of anthraquinone. Recrystallization from $CH_2Cl_2$/toluene at −30 °C afforded a red oily solid, which was washed with 30:40 petrol to give 100 mg (0.05 mmol, 93%) of red powder.

IR (KBr, cm$^{-1}$): 2553, 2531 (BH). $^1$H NMR ($C_6D_6$): $\delta$ −7.44 (s, Me), 0.38 (q, 4-C$H_2$CH$_3$), 0.58 (s, Me), 0.77 (t, 4-CH$_2$C$H_3$), 0.85 (t, 4-CH$_2$C$H_3$), 1.85 (t, 4-CH$_2$C$H_3$), 1.95 (q, 4-C$H_2$CH$_3$) 2.20 (q, 4-C$H_2$CH$_3$), 3.08 (s, Me), 3.24 (s, Me), 3.36 (s, Me), 3.40 (s, Me), 3.84 (s, C$_{14}$H$_8$O$_2$), 3.94 (s, C$_{14}$H$_8$O$_2$), 4.46 (s, Me), 4.63 (s, Me), 8.05 (s, C$_{14}$H$_8$O$_2$), 8.13 (s, C$_{14}$H$_8$O$_2$).

**Preparation of [Eu(Tp$^{Me2}$)$_2$(OC$_6$H$_4$O)], 8.** The compound was prepared as described for **6**, by reaction of 120 mg of [Eu(Tp$^{Me2}$)$_2$] (0.16 mmol) with 17 mg of 1,4-benzoquinone (0.16 mmol). Yield: 60% (82 mg, 0.1 mmol). Anal. Calcd for $C_{36}H_{48}N_{12}B_2O_2Eu$: C, 50.61; H, 5.66; N, 19.67. Found: C, 48.86; H, 5.76; N, 17.43. IR (Nujol, cm$^{-1}$): 2555, 2519 (sh) ($\nu_{B-H}$). $^1$H NMR (toluene-$d_8$, 20 °C): $\delta$ 10.59 (18H, br, Me-3), 1.36 (18H, Me-5), 0.85 (6H, H-4), 2.5 (2H, br, B−H).

**[Sm(Tp$^{Me2}$)$_2$(3,5-($^t$Bu)$_2$-o-O$_2$C$_6$H$_4$)], 9.** In a drybox, crystalline 3,5-di-*tert*-butyl-*o*-quinone (0.096 g, 0.436 mmol) was added slowly to a stirred purple suspension of **1** (0.325 g, 0.437 mmol) in THF. The reaction was immediate, and the color changed from purple to deep green as the insoluble Sm(Tp$^{Me2}$)$_2$ disappeared. After the reaction mixture had been stirred for 5 h, a trace amount of insoluble material was separated by centrifugation. The solvent was removed under reduced pressure, and a crystalline green solid was obtained. Recrystallization from diethyl ether gave analytically pure product (375 mg, 89%). Anal. Calcd for $C_{44}H_{64}B_2N_{12}O_2Sm$: C, 54.76; H, 6.68; N, 17.42. Found: C, 54.34; H, 6.94; N, 16.34. $^1$H NMR (toluene-$d_8$, −80 °C): $\delta$ 39.05 (s, 9H, C(C$H_3$)$_3$), 15.20 (s, 3H, C$H_3$), 11.60 (s, 3H, C$H_3$), 7.45 (s, 1H, 4-pz-*H*), 7.11 (s, 1H, 4-pz-*H*), 5.90 (s, 1H, 4-pz-*H*), 5.44 (s, 3H, C$H_3$), 4.89 (s, 1H, 4-pz-*H*), 4.50 (s$_{br}$, 9H, C(C$H_3$)$_3$), 4.18 (s, 1H, 4-pz-*H*), 3.56 (s, 3H, C$H_3$), 3.51 (s, 3H, C$H_3$), 3.44 (s, 3H, C$H_3$), 2.49 (s, 3H, C$H_3$), 2.45 (s, 3H, C$H_3$), 2.41 (s, 3H, C$H_3$), 2.35 (s, 3H, C$H_3$), 1.00 (s, 1H, 4-pz-*H*), −3.49 (s$_{br}$, 3H, CH$_3$), −4.11 (s$_{br}$, 3H, CH$_3$), −8.80 (s$_{br}$, 1H, *m*-Ar-*H*). $^{11}$B{$^1$H} NMR (toluene-$d_8$, 25 °C): $\delta$ −10.01, −10.67.

**X-ray Crystallographic Analysis.** Full details of major crystallographic parameters for each structure are reported in Table 2. Crystals **2**, **3**, and **6**, grown at low temperature from hexane, toluene, and toluene, respectively, were mounted in thin-walled glass capillaries within a nitrogen-filled glovebox. Data were collected at room temperature using an Enraf-Nonius CAD4-diffractometer with graphite-monochromated Mo K$\alpha$ radiation, using an $\omega-2\theta$ scan mode. The data were corrected[26] for Lorentz and polarization effects, for linear decay, and for absorption by empirical corrections based on $\psi$ scans. The heavy atom positions were located by Patterson methods using SHELXS-86.[27] The remaining atoms were located by successive least-squares refinements on $F^2$ using

(26) Fair, C. K. *MOLEN*; Enraf-Nonius: Delft, The Netherlands, 1990.
(27) Sheldrick, G. M. *SHELXS-86: Program for the Solution of Crystal Structure*; University of Göttingen: Göttingen, Germany, 1986.

**Table 2.** Crystallographic Data for Complexes for **2**·0.5$C_6H_8$, **3**·$C_7H_8$, **4**·$C_7H_8$, **6**·$C_7H_8$, **7**·2$CH_2Cl_2$, and **9**·0.5$C_7H_8$

| | **2**·0.5$C_6H_8$ | **3**·$C_7H_8$ | **4**·$C_7H_8$ | **6**·$C_7H_8$ | **7**·$CH_2Cl_2$ | **9**·0.5$C_7H_8$ |
|---|---|---|---|---|---|---|
| formula | $C_{46}H_{58}B_2N_{12}OSm\cdot0.5C_6H_8$ | $C_{50}H_{60}B_2N_{12}OSm\cdot C_7H_8$ | $C_{51}H_{72}B_2N_{12}O_2Sm$ | $C_{73}H_{100}B_4N_{24}O_2Sm_2$ | $C_{76}H_{100}B_4Cl_4N_{24}O_2Sm_2$ | $C_{47.5}H_{68}B_2N_{12}O_2Sm$ |
| fw | 973.02 | 1017.07 | 1057.18 | 1689.71 | 1867.54 | 1011.11 |
| cryst syst | triclinic | monoclinic | triclinic | triclinic | triclinic | triclinic |
| space group | $P\bar{1}$ | $P2_1/c$ | $P\bar{1}$ | $P\bar{1}$ | $P\bar{1}$ | $P\bar{1}$ |
| *a*, Å | 11.108(2) | 17.7840(10) | 10.924(2) | 14.8630(10) | 10.8129(16) | 13.110(14) |
| *b*, Å | 13.532(2) | 12.6480(10) | 15.040(3) | 17.717(2) | 14.0111(19) | 13.750(15) |
| *c*, Å | 17.7880(10) | 22.1080(10) | 18.785(4) | 17.932(2) | 14.493(2) | 14.698(12) |
| α, deg | 73.050(10) | | 89.96(3) | 87.510(10) | 102.135(4) | 92.42(2) |
| *β*, deg | 86.620(10) | 92.542(5) | 74.29(3) | 70.610(10) | 93.804(4) | 102.46(3) |
| *γ*, deg | 67.920(10) | | 71.14(3) | 69.940(10) | 91.768(4) | 104.53(1) |
| *V*, Å$^3$ | 2366.2(6) | 4967.9(5) | 2800(1) | 4170.7(7) | 2139.7(5) | 2491(4) |
| *Z* | 2 | 4 | 2 | 2 | 1 | 2 |
| *μ*, mm$^{-1}$ | 1.289 | 1.231 | 1.096 | 1.451 | 1.543 | 1.229 |
| *ρ*, g cm$^{-3}$ | 1.366 | 1.360 | 1.254 | 1.345 | 1.449 | 1.348 |
| R1[a] | 0.0395 | 0.0463 | 0.057 | 0.0708 | 0.0905 | 0.044 |
| wR2[b] | 0.0915 | 0.0951 | 0.137 | 0.1464 | 0.1488 | 0.097 |
| GOF | 1.110 | 1.045 | 1.012 | 1.055 | 0.995 | 1.059 |

[a] $R1 = \sum||F_o| - |F_c||/\sum|F_o|$. [b] $wR2 = [\sum(w(F_o^2 - F_c^2)^2)/\sum(w(F_o^2)^2)]^{1/2}$; $w = 1/[\sigma^2(F_o^2) + (aP)^2 + bP]$, where $P = (F_o^2 + 2F_c^2)/3$. The values were calculated for data with $I > 2\sigma(I)$.

SHELXL97.[28] The structural analysis of **6** revealed two halves of toluene molecules, severely disordered across two inversion centers and were refined as benzene molecules, ignoring the methyl group. All the non-hydrogen atoms were refined anisotropically, except the solvent atoms. Atomic scattering factors and anomalous dispersion terms were taken as in ref 28. The drawings were made with ORTEPII,[29] and all the calculations were performed on a DEC α 3000 computer.

Diffraction data were collected at 293 K for a red single-domain crystal of **4**·$C_7H_8$, grown from toluene solution at low temperature, using graphite-monochromated Mo Kα radiation ($\lambda = 0.71073$ Å) and full (1.10° wide) $\omega$ scans on a Syntex P $\bar{1}$ autodiffractometer. The data were corrected empirically for variable absorption effects using $\psi$ scans for six reflections before application of Lorentz and polarization corrections. The Bruker AXS software package SHELXTL[30] was used to solve the structure using "direct methods" techniques. The resulting structural parameters were refined using $F_o^2$ data with weighted (SHELXTL) full-matrix least-squares techniques on a Pentium PC computer. Atoms of the metal complex are ordered, but those of the two crystallographically independent half toluene solvent molecules of crystallization are severely disordered. Each of these toluene molecules is disordered about a (different) crystallographic inversion center. Only the ring carbon atoms could be located, and they were included in the structural model as isotropic half-occupancy carbon atoms located at the vertices of a regular hexagon with an edge length of 1.39 Å. The methyl groups for these toluene molecules could not be located. The final structural model for **4**·$C_7H_8$ incorporated anisotropic thermal parameters for all nonhydrogen atoms in the metal complex and isotropic thermal parameters for all included carbon atoms of the toluene solvent molecules of crystallization. All hydrogen atoms of the metal complex were included in the final structural model as idealized isotropic atoms; hydrogen atoms were not included for the toluene solvent molecules of crystallization.

X-ray quality crystals of **7** were grown from dichloromethane/THF solution as red plates. A crystal for **7** was mounted on a glass fiber in an oil drop, and data were collected on a Bruker AXS SMART 1K CCD area detector diffractometer at 160 K with narrow frames (0.3° in $\omega$) and a three-dimensional profile fitting using graphite-monochromated Mo Kα radiation ($\lambda = 0.71073$ Å). Data were corrected for Lp effects and semiempirically for absorption based on symmetry-equivalent and repeated reflections. The structure was solved by direct methods and refined by full-matrix least-squares on $F^2$ values. All non-H atoms were refined anisotropically. H atoms were constrained. The molecule lies on an inversion center. Programs: Bruker AXS SHELXTL[30] for structure solution and refinement and molecular graphics, Siemens/Bruker AXS SMART (control), and SAINT (integration) and local programs.[31]

For **9**, a crystal was mounted under argon in a glass capillary. Data were collected by Dr. J. F. Britten (Department of Chemistry, McMaster University, Hamilton, ON, Canada L8S 4M1). Data were collected at 213 K using a Siemens P4/RA diffractometer/SMART 1K CCD area detector combination using graphite-monochromated Mo Kα radiation ($\lambda = 0.71073$ Å), with narrow-scan frames (0.3° in $\omega$) and three-dimensional profile fitting. Data were corrected for Lp effects and semiempirically for absorption by multiscan methods using SADABS. The structure was solved using direct methods (SHELXS-86).[27]Least-squares structure refinement (on $F^2$) was completed using SHELXL-97.[28]All non-H atoms were refined anisotropically. H atoms were constrained. All calculations were carried out using an IBM-compatible personal computer running Windows 2000.

**Acknowledgment.** Financial support from PRAXIS XXI (2/2.1/QUI/386/74) (NM), the Natural Sciences and Engineering Research Council of Canada and the University of Alberta (J.T.), and from NATO (N.M. and J.T.) is gratefully acknowledged. I.L. thanks PRAXIS XXI for a PhD grant. A.S. wishes to thank the EPSRC for a studentship in support of ACH.

**Supporting Information Available:** CIF files with details of the X-ray structures of complexes **2**−**4**, **6**, **7**, and **9** and a detailed experimental for the determination of **4**. This material is available free of charge via the Internet at http://pubs.acs.org.

IC701364K

(28) Sheldrick, G. M. *SHELXL-97: Program for the Crystal Structure Refinement*; University of Göttingen: Göttingen, Germany, 1997.
(29) Johnson, C. K. *ORTEPII*; Report ORNL-5138; Oak Ridge National Laboratory; Oak Ridge, TN, 1976.
(30) Sheldrick, G. M. *SHELXTL User Manual*, version 5; Bruker AXS Inc.: Madison, WI, 1994.
(31) *SMART and SAINT software for CCD diffractometers*; Bruker AXS, Inc.: Madison, WI, 1994.